Nuclear Instruments and Methods in Physics Research B 267 (2009) 3080–3083

Contents lists available at ScienceDirect

Nuclear Instruments and Methods in Physics Research B

journal homepage: www.elsevier.com/locate/nimb

Molecular simulations of cluster ejection by CO_2 cluster impact on carbon-based surfaces

Tomohiro Shinya [a], Hiroaki Kirihata [a], Yasutaka Yamaguchi [a,*], Hisato Yasumatsu [b], Tamotsu Kondow [b], Herbert M. Urbassek [c], Jürgen Gspann [d]

[a] Department of Mechanical Engineering, Osaka University, 2-1 Yamadaoka, Suita 565-0871, Japan
[b] Cluster Research Lab., Toyota Technological Institute: in East Tokyo Lab., Genesis Research Institute, Inc., 717-86 Futamata, Ichikawa 272-0001, Japan
[c] Fachbereich Physik, Universität Kaiserslautern und Forschungszentrum OPTIMAS, P.O. Box 3049, Erwin-Schrödinger-Straße, 67663 Kaiserslautern, Germany
[d] Institut für Mikrostrukturtechnik, Universität und Forschungszentrum Karlsruhe, P.O. Box 3640, 76021 Karlsruhe, Germany

ARTICLE INFO

Article history:
Available online 16 June 2009

PACS:
79.20.Rf
79.20.AP
61.80.Lj

Keywords:
Cluster impact
Carbon-based surface
Reactive sputtering
Collision cascade

ABSTRACT

Single $(CO_2)_N$ (N = 1–20) cluster impact on three different carbon-based surfaces of fullerite (1 1 1), graphite and diamond (1 0 0) has been investigated by MD simulations with the cluster collision energy from 5 to 14 keV/cluster as a first step toward the general modeling of the reactive sputtering by cluster impact of a solid surface. A crater permanently remained on the fullerite and graphite surfaces while it was quickly replenished with fluidized carbon material on the diamond surface. In spite of the smaller crater size as well as the crater recovery resulting in the reduction of the surface area, the sputtering yields were the highest on diamond. The effective energy deposition near the surface contributes to the temperature rise and consequent sputtering seemed highly reduced due to the collision cascades especially on the fullerite target.

1. Introduction

Cluster ion beam is a novel method for surface modification in nano-scale, such as surface smoothing, sputtering and shallow implantation [1–5]. The authors have applied highly accelerated ionized cluster beams for micro- and nano-scale surface structuring [6–9], where $(CO_2)_N$ or Ar_N ($N \sim 1000$) clusters continuously impact on the diamond surface at a cluster collision energy $E_{col}^{cluster}$ up to 100 keV/cluster. The reactive enhancement of the surface erosion was clearly observed in the higher erosion rate with $(CO_2)_N$ impact with a factor of 3.63 than that with Ar_N impact, while the eroded surface was remarkably smoother for the Ar_N impact [8,9]. Based on this experiment, we have performed molecular dynamics (MD) simulations of single $(CO_2)_N$ and Ar_N ($N \sim 1000$) cluster impacts on a diamond (1 1 1) and (1 0 0) surfaces with an $E_{col}^{cluster}$ up to 100 keV [10–13], and showed the differences in the sputtering yields with a factor about 3.5 at $E_{col}^{cluster}$ = 100 keV as well as the surface roughness after the impact. The enhancement in the erosion became remarkable only for $E_{col}^{cluster}$ above 75 keV. In addition, further comparison with $(C_3)_N$ and $(O_2)_{1.5N}$ impacts revealed that a significant erosion effect was achieved from $E_{col}^{cluster}$ = 30 keV using $(O_2)_{1.5N}$, and these differences were ascribed to the reactive emission pattern via the production of CO and CO_2 molecules [12].

Recently, we have also experimentally performed size-selected $(CO_2)_N^+$ (N = 1–25) impact on graphite at $E_{col}^{cluster}$ ranging from 5 to 14 keV [14,15], and revealed that the mass spectroscopy of the ejected carbon cluster anions C_m^- (m = 1–12) agreed well with MD simulation results [15]. The $E_{col}^{cluster}$ dependence of the sputtering yield there for larger clusters were explained well by the thermal desorption model as:

$$N_{sput} \propto S \exp\left(-\frac{E_d}{kT}\right), \quad kT = \gamma \frac{E_{col}^{cluster}}{3\rho_n S d} \tag{1}$$

assuming that the yield was determined from the crater surface area S, desorption barrier E_d, and instantaneous temperature T, which was given by the efficient energy deposition in a local volume around the impact point expressed using the efficiency γ, crater depth d, number density ρ_n around the crater and Boltzmann constant k as well [15]. The inconsistency for smaller clusters ($N \leqslant 5$) apparently arose when the binary collision sequence known as the 'collision cascades' were induced in the target at higher collision energies, i.e. higher velocities.

For the further modeling and toward the general understanding of the reactive sputtering by a cluster impact on a solid surface, single $(CO_2)_N$ (N = 1–20) impacts on typical carbon-based surfaces

* Corresponding author. Tel.: +81 6 6879 7251; fax: +81 6 6879 7255.
E-mail address: yamaguchi@mech.eng.osaka-u.ac.jp (Y. Yamaguchi).

0168-583X/$ - see front matter © 2009 Elsevier B.V. All rights reserved.
doi:10.1016/j.nimb.2009.06.021

of fullerite (C_{60} crystal) (1 1 1), graphite and diamond (1 0 0) are investigated by MD simulations in this study.

2. Method

The simulation methods are basically the same as in our previous reports [10–13,15,16]. Briefly, the empirical potential function proposed by Brenner [17] with the parameter set I is adopted for the interaction among carbon atoms with a slight simplification [18], while the interaction potentials of C–O and O–O are derived appropriately from Brenner's formula [10]. The long-range intervan der Waals force are included as the 12–6 Lennard–Jones (L-J) acting between carbon atoms in different covalent networks with a transition barrier using a cut-off screening function [15,16] in order to reduce unrealistic strong repulsion between graphene sheets in graphite and between C_{60}S in fullerite in a short distance range. This long-range interaction is applied only for the impact simulations on graphite and fullerite.

The target conformation is also basically the same as in our previous reports [10–13,15,16]. For the fullerite target, the (1 1 1) surface of a C_{60} crystal is modeled with a rounded hexagonal pyramid shape, and the target consisting of 1708 C_{60} molecules, i.e. 102480 carbon atoms, and the depth and the length of the lateral diagonal line are 81 and 187 Å, respectively. The center of mass of the outermost C_{60} molecules is connected to their initial equilibrium position with an additional virtual spring so that the target far from the impact point keeps the proper crystal shape. The spring constant k = 15 N/m is derived from the second derivative of the mean potential change around the equilibrium point. Except for this fullerite target with a rather specific conformation, cylindrical structure is applied as the impact target of graphite and diamond (1 0 0) surface. The number of carbon atoms ranges from about 140000 to 270000 and 130000 to 350000 for graphite [15] and diamond targets, respectively depending on the impact energy.

The side and bottom boundaries of the graphite and diamond targets are fixed, and the boundary temperature is maintained at 300 K with the Langevin method [13,15], while the temperature control is enforced on the outermost C_{60} molecules with the Langevin method at 300 K, where the inter-vibration as the motion of the center of mass of C_{60} molecules is also controlled with the Debye temperature θ = 50 K as well as the intra-C_{60} vibration controlled with θ = 420 K.

Geometric structures of the projectile, $(CO_2)_N$ (N = 1, 5, 7, 10, 15 and 20), were obtained by annealing each cluster at 40 K with an additional inter Lennard–Jones force [10]. Numbers of simulation runs are about 10 for each impact so as to obtain statistical data from the multiple runs with changing the impact location in the surface as well as the cluster orientation randomly.

Verlet's method is adopted to integrate the equation of motion, and the time step was changed depending on the maximum velocity of the atoms [15]. Each simulation ran for 8 ps except for several impact simulations on fullerite to investigate the long timescale feature.

3. Results and discussion

Fig. 1 shows the snapshots of the $(CO_2)_{20}$ impacts on fullerite (1 1 1), graphite and diamond (1 0 0) surfaces at a cluster collision energy $E_{col}^{cluster}$ of 14 keV/cluster. Cross sections parallel to the impact direction with the thickness of 10 Å is exhibited, and the brightness of carbon atoms corresponds to the temperature. As a remarkable difference in the early stage of the impact, the collision cascades can be seen as rather arbitrary distributing dark shades only on fullerite in Fig. 1(a-i) while clear ordered propagating shockwave structures are observed in graphite (Fig. 1(b-ii)) and diamond (Fig. 1(c-i)). The crater simultaneously formed at this stage remain permanently in fullerite (Fig. 1(a-iv)) and graphite (Fig. 1(b-iv)), and several sputtered species still stay in the crater in graphite, while the crater is quickly replenished with the fluidized carbon material around the impact point in diamond (Fig. 1(c-iii)). This crater replenishment was also observed in the case of large $(CO_2)_N$ and Ar_N ($N \sim 1000$) impact on diamond [10–13]. The temperature around the impact point has already been decreased down on graphite and diamond indicated as bright shades in Fig. 1(b-iv) and (c-iv) due to the high thermal conductivity, while the impact point is still hot at 4 ps seen as relatively dark shades

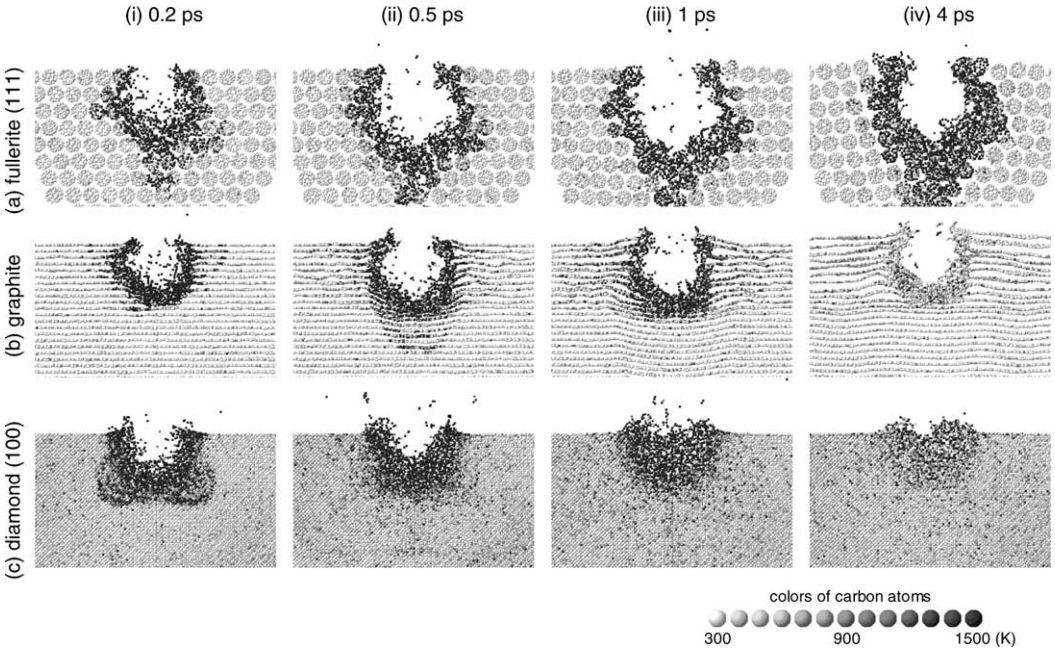

Fig. 1. Snapshots of $(CO_2)_{20}$ impacts on fullerite (1 1 1), graphite and diamond (1 0 0) surfaces at a cluster collision energy of 14 keV. Cross sections parallel to the impact direction with the thickness of 10 Å are exhibited and the brightness of carbon atoms corresponds to the temperature.